

CHEMICAL PHYSICS

Conformer-specific photochemistry imaged in real space and time

E. G. Champenois^{1†}, D. M. Sanchez^{1,2†}, J. Yang^{1,3,4}, J. P. Figueira Nunes⁵, A. Attar³, M. Centurion⁵, R. Forbes³, M. Gühr⁶, K. Hegazy^{1,7}, F. Ji³, S. K. Saha⁵, Y. Liu⁸, M.-F. Lin³, D. Luo³, B. Moore⁵, X. Shen³, M. R. Ware¹, X. J. Wang^{3,*}, T. J. Martínez^{1,2,*}, T. J. A. Wolf^{1*}

Conformational isomers (conformers) of molecules play a decisive role in biology and organic chemistry. However, experimental methods for investigating chemical reaction dynamics are typically not conformer-sensitive. We report on a gas-phase megaelectronvolt ultrafast electron diffraction investigation of α -phellandrene undergoing an electrocyclic ring-opening reaction. We directly imaged the evolution of a specific set of α -phellandrene conformers into the product isomer predicted by the Woodward-Hoffmann rules in real space and time. Our experimental results are in quantitative agreement with nonadiabatic quantum molecular dynamics simulations, which provide considerable detail of how conformation influences the time scale and quantum efficiency of photoinduced ring-opening reactions.

Conformational isomers, or conformers, can interconvert via rotations around single chemical bonds. Interconversion between conformers represents an important step in many bimolecular reactions, where reactant species must encounter one another not only in a particular orientation but also in a specific structural conformation (1). Moreover, conformer dynamics arise naturally in self-ordering of macromolecular structures (e.g., protein folding) (2). However, investigation of conformer-specific dynamics on their natural time and length scales of femtoseconds and angstroms is hindered by the insensitivity of established experimental methods to conformers.

The influence of conformers on photochemical reactivity is well known, such as from electrocyclic reactions according to the Woodward-Hoffmann (WH) rules (3). These rules predict them to be concerted and conformer-specific (i.e., leading to different reaction products depending on the reactant conformer). Moreover, the WH rules predict an inverted conformer specificity for electrocyclic ring opening in the electronically excited state versus the ground state of a molecule. Electrocyclic reactions play an important role in chemical synthesis (4) and vitamin D production in human skin (5).

An instructive example of conformer specificity is the photochemical ring opening of the monoterpene α -phellandrene (α PH) (6), which is produced by plants and used in the fragrance, food, and pharmaceutical industries (7). α -Phellandrene consists of a 1,3-cyclohexadiene (CHD)-like ring moiety with two substituents: an isopropyl group at its sp^3 -hybridized C_1 position and a methyl group at the C_8 position (Figs. 1 and 2). The substitution gives rise to two conformers with the isopropyl group being in either quasi-axial (ax) or quasi-equatorial (eq) orientation (i.e., approximately perpendicular or parallel to the ring plane, respectively). The WH rules predict the ring opening to take place in a concerted, conrotatory motion; that is, both ends of the newly formed open-ring molecule rotate away from each other in the same clockwise or counterclockwise direction (Fig. 1A). This motion leads to different photoproducts depending on the reactant conformer: the isomers (3Z,5E)-3,7-dimethylocta-1,3,5-triene (ZEDOT, from eq- α PH) and (3Z,5Z)-dimethylocta-1,3,5-triene (ZZDOT, from ax- α PH) (Fig. 1).

Evidence for the conformer specificity of the ring opening in α PH (6) and other reactants (8, 9) has been observed in solution-phase measurements of photoproduct ratios. Moreover, resonance Raman investigations revealed evidence for the importance of conrotatory motion in the depopulation of the Franck-Condon region of the reactant excited state (10). The photochemical dynamics leading from the Franck-Condon region to the ring-opened photoproducts of α PH have been investigated by several ultrafast spectroscopic studies in both the gas and condensed phase, although largely without sensitivity to the structural dynamics, reactant conformers, or photoproduct isomers (11–15).

Here, we report on a combined megaelectronvolt ultrafast electron diffraction (UED) and ab initio multiple spawning (AIMS) (16–18) study of conformer-specific dynamics in the photochemical ring opening of gas-phase α PH

with unambiguous conformer sensitivity, confirming but going far beyond the qualitative orbital symmetry-based WH rule predictions. In both our static diffraction measurements and quantum chemical calculations, we found the eq- α PH conformer to dominate in our gas-phase sample (text SI). As opposed to other studies of electrocyclic reactions, our time-resolved measurements directly image concerted and exclusive formation of the ZEDOT photoproduct predicted by the WH rules on the femtosecond time scale with sub-angstrom resolution and in quantitative agreement with AIMS simulations of the photochemical dynamics.

The simulations reveal that after photoexcitation into the lowest excited state (S_1) with $\pi\pi^*$ character, α PH nonadiabatically relaxes to the electronic ground state (S_0) through three different conical intersection (CI) geometries (19). Only one of them yields ring-opened photoproducts; the other two form vibrationally “hot” reactants. The presence of the isopropyl group redirects significant ($40 \pm 4\%$) amounts of the S_1 population toward the non-WH CIs, substantially reducing the WH-photoproduct yield relative to CHD (20). Additionally, the rotational orientation of the isopropyl group gives rise to three rotational conformers (rotamers) for each of the eq- and ax- α PH structures, labeled as gauche+/- (G+/G-) and trans (T) (Fig. 2), which were simultaneously present in our sample. These rotamers show different ring-opening time scales.

Identification of the reactant conformer

Figure 2A shows the extracted static atomic pair distribution function [PDF(r)] from a gas-phase sample of randomly oriented α PH molecules. For comparison, we plotted simulated PDFs of all six ax- α PH/eq- α PH rotamer geometries. We analyzed the structural information contained in the PDFs in terms of carbon coordination shells, which are additionally plotted as bars for the eq- α PH (blue) and ax- α PH (red) conformers in Fig. 2A: The many C-C bonds (first carbon coordination shell, labeled as α) in the system give rise to a strong maximum in all PDFs at 1.4 Å. A second peak at 2.4 Å corresponds to the second carbon coordination shell (the distances between carbon atoms two atomic sites away from each other; β in Fig. 2A) with some contributions from the third coordination shell (distances of carbons three atomic sites apart from each other). The signatures above 3 Å belong to the third and higher coordination shells.

We found the strongest differences between the PDFs within the third coordination shell (γ in Fig. 2A). All eq- α PH rotamers, the ax-G- α PH rotamer, and the experimental PDF exhibit a minimum around 3.5 Å, in contrast to the two remaining ax- α PH rotamers that produce a shoulder. The minimum results from a splitting of the third coordination shell in the eq- α PH and ax-G- α PH rotamers into

¹Stanford PULSE Institute, SLAC National Accelerator Laboratory, Menlo Park, CA, USA. ²Department of Chemistry, Stanford University, Stanford, CA, USA. ³SLAC National Accelerator Laboratory, Menlo Park, CA, USA. ⁴Center of Basic Molecular Science, Department of Chemistry, Tsinghua University, Beijing, China. ⁵Department of Physics and Astronomy, University of Nebraska, Lincoln, NE, USA. ⁶Institut für Physik und Astronomie, Universität Potsdam, Potsdam, Germany. ⁷Department of Physics, Stanford University, Stanford, CA, USA. ⁸Department of Physics and Astronomy, Stony Brook University, Stony Brook, NY, USA. *Corresponding author. Email: thomas.wolf@stanford.edu (T.J.A.W.); toddmartinez@gmail.com (T.J.M.); wangxj@slac.stanford.edu (X.J.W.)

†These authors contributed equally to this work.

‡Present address: Design Physics Division, Lawrence Livermore National Laboratory, Livermore, CA, USA.

distances between carbons in cis configuration (small dihedral angles, $3c$ in Fig. 2A) (e.g., the C_3 - C_9 distance) and in trans configuration (large dihedral angles, $3t$ in Fig. 2A) (e.g., the C_3 - C_{10} distance). The splitting collapses for the ax-G+ and ax-T rotamers because one of the methyl groups of the isopropyl substituent is directly below the carbon ring and thereby moves many of the ring carbon-methyl carbon distances into the γ region (see structures in Fig. 2). The high level of agreement of the experimental PDF with those of eq- α PH and disagreement with some of the ax- α PH PDFs suggest that the sample is dominated by eq- α PH rotamers, in agreement with our quantum chemical calculations (text S1) and previous results (21).

Evolution into the Woodward-Hoffmann predicted product isomer

Figure 2B shows an experimental Δ PDF 260 fs after photoexcitation with an ultrashort 266-nm optical pulse (experimental instrumental response function: 150 fs full width at half maximum; see supplementary materials). Atomic distance changes appear in Δ PDFs as a combination of a negative contribution at the initial atomic distance and a positive contribution at the delay-dependent distance. Accordingly, the experimental Δ PDF in Fig. 2B shows signatures from ring opening. The negative signature in the α region directly follows from

breaking the C_1 - C_4 bond. The negative signature in the β region mainly results from increases in the C_1 - C_9 , C_2 - C_4 , and C_3 - C_4 distances. Positive signatures in the γ region suggest that at least some of these distances increase to values close to 3.5 Å. The structural implications of these distance changes can be qualitatively understood by comparison to “simple” Δ PDF simulations generated from single photoproduct and reactant geometries. Such simulations for the WH-predicted photoproducts of eq- α PH \rightarrow ZEDOT (blue line) and ax- α PH \rightarrow ZZDOT (red line) are plotted in Fig. 2B. Additionally, the WH-forbidden reactant \rightarrow photoproduct Δ PDF simulations of eq- α PH \rightarrow ZZDOT (blue dashes) ax- α PH \rightarrow ZEDOT (red dashes) are shown. Similar to the static PDFs, experimental and simulated Δ PDFs show the most prominent differences in the γ region. Differences between experimental and simulated Δ PDFs in the α and β regions are due to the approximation of the photoproduct by a single geometry. The WH-allowed photoproduct of the eq conformers shows good qualitative agreement with a strong positive signature in the γ -region of the experimental Δ PDF, whereas all other photoproduct Δ PDFs show essentially zero or negative amplitude.

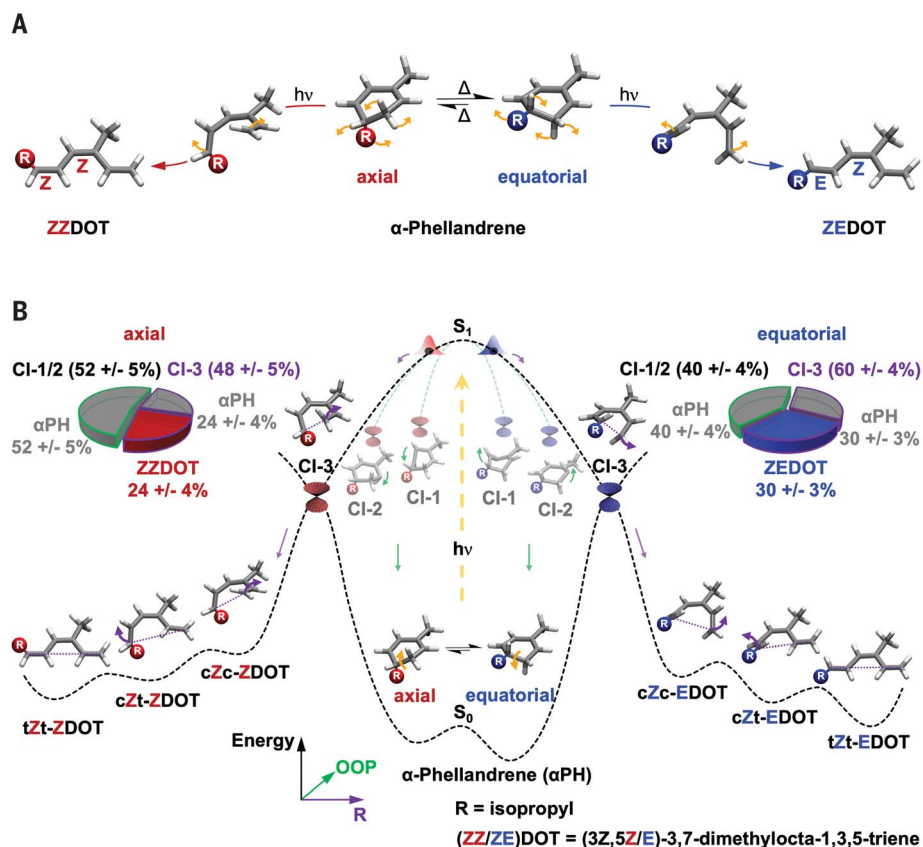
The difference between the simulated photoproduct Δ PDFs can be explained by steric effects from the bulky isopropyl group: In

eq- α PH, it points away from the carbon ring. The WH-predicted conrotatory motion (Fig. 1A) rotates it farther away, favoring smaller atomic distance changes into the γ region in the photoproduct (e.g., the cZc-EDOT geometry in Fig. 1B). In ax- α PH, the WH-predicted conrotatory motion rotates the isopropyl group into the carbon ring. This is sterically unfavorable, forcing larger atomic distance changes beyond the γ region in the photoproduct (e.g., the tZt-ZDOT geometry in Fig. 1B). Thus, both effects—the positive signature of eq- α PH \rightarrow ZEDOT and the negative signature of ax- α PH \rightarrow ZZDOT—are direct results of the orientation of the isopropyl group in the reactant conformer and therefore an unambiguous signature of conformer-specific ring opening.

Figure 3 shows a comparison of experimental Δ PDFs with those computed from AIMS simulations (18) using α state-averaged complete active-space self-consistent field theory (α -CASSCF) (22). Experimental Δ PDFs are shown as lineouts in Fig. 3B and as a false-color plot in Fig. 3E. The simulated Δ PDFs of the individual G-, T, and G+ rotamers are averaged assuming roughly equal contributions at room temperature and plotted analogously to the experimental Δ PDFs in Fig. 3, A and D, for eq- α PH and in Fig. 3, C and F, for ax- α PH. Additionally, the delay-dependent integrated experimental Δ PDFs in the α , β , and γ regions

Fig. 1. Conformer-specific photochemistry in α -phellandrene.

(A) Woodward-Hoffmann predictions for the conformer specificity of photoinduced electrocyclic ring opening in α -phellandrene. Its isopropyl substituent (R) can be in axial or equatorial orientation with respect to the carbon ring. Axial and equatorial conformers are in thermal equilibrium in solution phase (Δ). (6) The Woodward-Hoffmann rules predict a concerted, conrotatory ring-opening motion (orange arrows) yielding isomers with R in different positions depending on the reactant conformer. (B) Schematic based on ab initio multiple spawning simulations of the photoinduced ring opening. Equatorial and axial conformers are photoexcited from their respective ground-state (S_0) energy minima to the first excited state (S_1); they evolve along an out-of-plane (OOP, green) coordinate toward conical intersections CI-1 and CI-2 or along the ring-opening coordinate (purple) toward CI-3. CI-1 and CI-2 lead to reformation of α -phellandrene, whereas CI-3 leads to both α PH reformation and ring opening. Several different conformers of the ZZDOT/ZEDOT photoproduct minima (cZc, cZt, and tZt) are accessible in the ground state. The two pie charts visualize the photoproduct distribution for axial and equatorial conformers as well as the distribution among the CI geometries CI-1 to CI-3; errors representing 68% confidence intervals were obtained from bootstrap analysis.



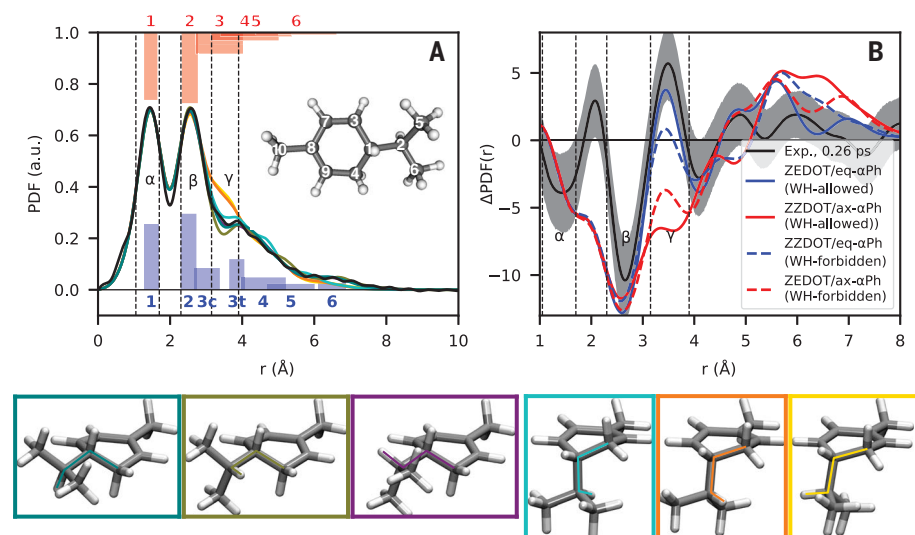


Fig. 2. Comparison of experimental and simulated structural information. (A) Experimental (black) and simulated pair distribution functions PDF(r) of six α -phellandrene (α PH) conformers, which are depicted below together with the dihedral angles defining the rotation of the isopropyl group [two gauche orientations (G+/G-) and one trans (T) orientation of the marked isopropyl hydrogen with respect to the marked ring carbon]. Carbon-carbon coordination spheres for axial (red) and equatorial (blue) conformers are shown as bars. Additionally, the α , β , and γ ranges of Fig. 3 are shown. The inset shows the carbon atom numbering used in the text. (B) Experimental difference PDF [Δ PDF(r)] at a pump-probe delay of 0.26 ps (black) and simple simulations of the signature of Woodward-Hoffmann (WH)-allowed and WH-forbidden reaction product signatures of the equatorial (eq- α PH) and axial (ax- α PH) reactant conformers and (3Z,5E)-3,7-dimethylocta-1,3,5-triene (ZEDOT) and (3Z,5Z)-dimethylocta-1,3,5-triene (ZZDOT) product isomers. Shaded areas represent a 68% confidence interval obtained from bootstrap analysis.

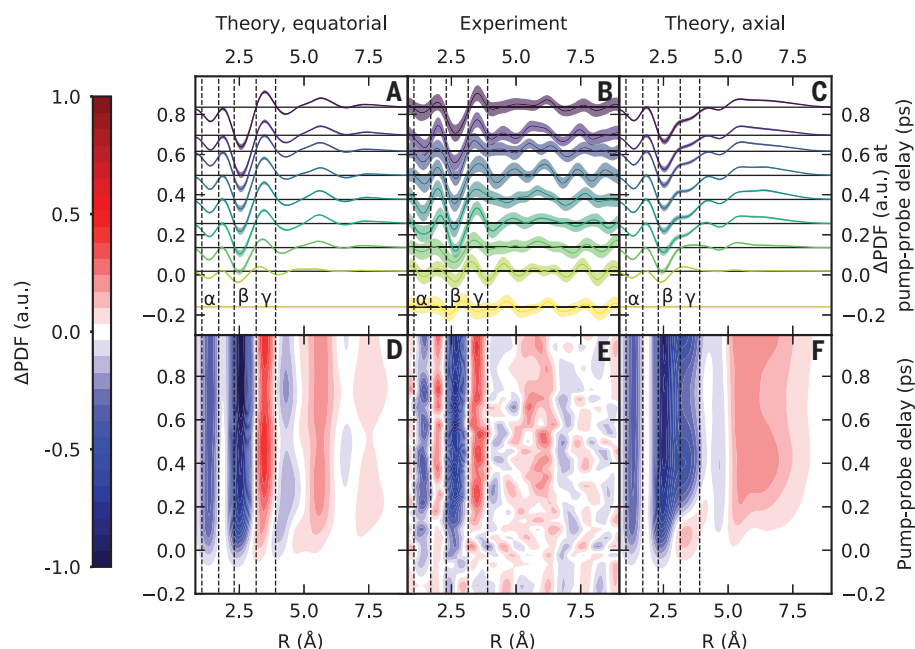


Fig. 3. Comparison of experimental and simulated time-dependent difference pair distribution functions (Δ PDF) of equatorial and axial conformers. (A–C) Δ PDFs at different pump-probe delays. (D–F) False-color plots of Δ PDF over the whole investigated time window of 1.2 ps. Simulated Δ PDFs are based on ab initio multiple spawning simulations (see supplementary materials) and represent the averaged dynamics of the G+, G-, and T rotamers. Shaded areas [(A) to (C)] represent a 68% confidence interval obtained from bootstrap analysis. For the simulations, these error bars reflect convergence with respect to initial condition sampling.

are compared in Fig. 4 with the corresponding curves for the averaged and individual eq- α PH rotamer contributions. The averaged AIMS Δ PDFs of the eq conformers show quantitative agreement with the experimental data within their limited signal-to-noise level. The averaged AIMS Δ PDFs of the ax conformers qualitatively disagree with the experimental data in the γ region. The experimental time-dependent signatures are clearly dominated by the eq- α PH rotamers (>80%; see text S1). Thus, we unambiguously observed exclusive formation of the WH-predicted photoproducts of the eq- α PH conformer within a few hundred femtoseconds after optical excitation. Our results constitute direct observation of conformer-specific photochemical reaction dynamics in real space and time.

Conformer-specific dynamics beyond the Woodward-Hoffmann rules

Our AIMS simulations revealed additional aspects of the relaxation process that could not be easily extracted from the experimental data. α -Phellandrene relaxes via the WH-predicted conrotatory ring-opening motion through a CI (CI-3) yielding both ring-opened photoproducts and the closed-ring reactant (Fig. 1B, Fig. 5A, and fig. S2). As a consequence of its differential nature, the Δ PDF observable is preferentially sensitive to the part of the population undergoing ring opening. Additionally, out-of-plane bending in S_1 leads through two CIs (CI-1/CI-2) to the closed-ring reactant (table S1). Furthermore, we observed a hitherto unknown secondary ring-closure reaction in the electronic ground state, yielding 2-ladderane (5-isopropyl-2-methylbicyclo[2.2.0]hex-2-ene). The ring closure was exclusively observed for the fraction of population undergoing internal conversion through CI-1 in the ground state (text S2). Non-WH relaxation pathways have been observed before for the prototypical CHD molecule (23) but had marginal contributions to the relaxation process. The presence of the isopropyl substituent redirects $40 \pm 4\%$ of the eq- α PH S_1 population toward non-WH pathways and thus substantially reduces the ring-opening quantum yield (Fig. 1B).

The time dependence of the measured and computed Δ PDFs in the α , β , and γ regions are shown in Fig. 4 and fig. S3B for the eq and ax conformers, respectively. The averaged simulation assuming equal distribution of the three eq rotamers (G-, T, and G+) leads to quantitative agreement with experiment, whereas individual eq rotamer contributions to the Δ PDFs are quite distinct (Fig. 4). Thus, the rotational orientation of the isopropyl group must influence the mechanism and time scale of ring opening. This fact becomes obvious in Fig. 5B, top, where simulated nonadiabatic population transfer events are categorized with respect to their C_1 - C_4 distances at the time of the transfer event—that is, their ability to undergo ring

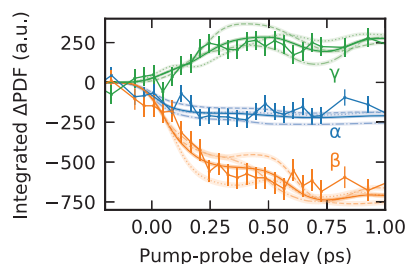


Fig. 4. Comparison of integrated difference pair distribution functions (Δ PDF) from experiment and simulations in the α , β , and γ regions of Fig. 3.

Experimental signals (dots with error bars) are compared to corresponding signals of the averaged (lines) and the individual equatorial rotamer simulations with the isopropyl group in gauche+ (G+, dashed lines), gauche- (G-, dotted lines), and trans (T, dash-dotted lines) orientations. The experimental error bars and the shaded areas around the line plots of the simulations represent a 68% confidence interval obtained from bootstrap analysis. For the simulations, these error bars reflect convergence with respect to initial condition sampling.

opening and thus to contribute to the Δ PDF observable (see above). In the case of the eq-G-rotamer, almost all of the population undergoing ring opening relaxes to S_0 within 200 fs after photoexcitation. The other two rotamers show substantially less ring opening in this time frame. Their remaining population undergoes ring opening considerably later, 500 to 700 fs after photoexcitation. The difference in ring-opening time scale is clearly reflected in the time-dependent Δ PDF amplitudes in Fig. 4.

Conclusion

By combining UED with AIMS simulations, we directly observed conformer-specific photochemical reaction dynamics on their natural time and length scales in agreement with the Woodward-Hoffmann rules. Moreover, we observed considerable effects on the efficiency and time scale of the reaction from the presence and orientation of an isopropyl substituent of the molecule. Similar conformer-dependent photochemistry has been observed only in a limited number of studies of photoproduct distributions, mostly after conformer-specific resonance-enhanced photoionization (1, 24–26). Because organic structures are prone to a large number of ground-state conformers and rotamers, our findings could have a large impact on our understanding of photochemical reaction mechanisms. We speculate that the paucity of previous observations of conformer and rotamer specificity is due to the absence of suitable experimental observables and challenges in preparing conformer-pure samples. Our study now demonstrates a suitable experimental observable. The investigation of specific conformers can be facilitated by methodological develop-

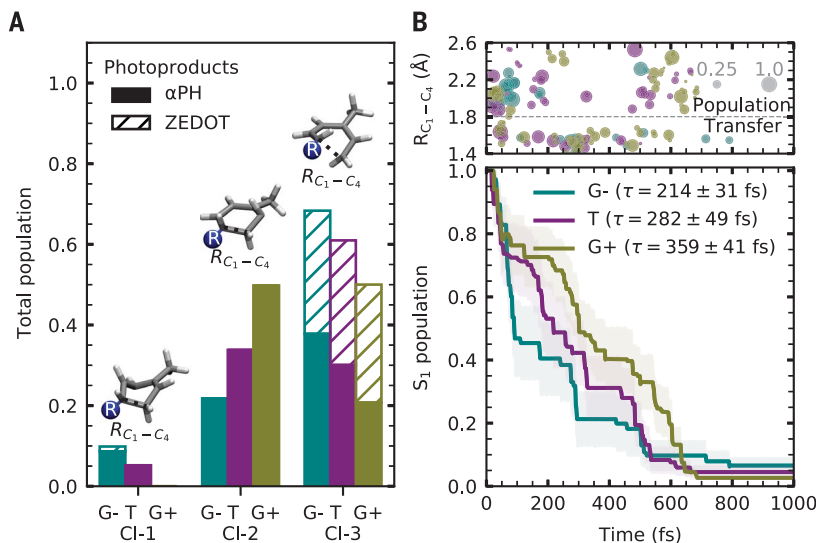


Fig. 5. Characterization of the closed- and open-ring nonradiative relaxation pathways of equatorial (eq) rotamers. (A) Histogram of the branching ratio between the closed and open pathways from simulations. Solid and hatched bars represent fractional populations that reform α -phellandrene (α PH) or ZEDOT, respectively. The insets show the minimum geometries of the conical intersections (CI) 1 to 3 of α PH, with the isopropyl substituent depicted as R. Additionally, the C_1 - C_4 distance ($R_{C_1-C_4}$, Fig. 2A) is marked. (B) Top: $R_{C_1-C_4}$ versus population transfer time in femoseconds from the excited state (S_1) to the ground state (S_0) for all 45 equatorial initial conditions (see supplementary materials). The black dashed line corresponds to the threshold used to determine whether the ring is open or closed. The circle radius is proportional to the amount of population involved in the transfer event and separated into the three rotamers. Bottom: The S_1 population decay for the three eq-rotamers with the isopropyl group in gauche (G+/G-) or trans (T) orientation in the first picosecond after photoexcitation. Shaded areas represent a 68% confidence interval obtained from bootstrap analysis.

ments in the area of conformer-selected molecular beams (27, 28) and single-molecule methods such as Coulomb explosion imaging (29) in combination with high-repetition rate x-ray free electron laser sources. Future investigations of photochemical dynamics using such emerging methods will provide general access to conformer-specific photochemistry.

REFERENCES AND NOTES

- Y.-P. Chang *et al.*, *Science* **342**, 98–101 (2013).
- K. A. Dill, J. L. MacCallum, *Science* **338**, 1042–1046 (2012).
- R. B. Woodward, R. Hoffmann, *Angew. Chem. Int. Ed.* **8**, 781–853 (1969).
- T. Bach, J. P. Hehn, *Angew. Chem. Int. Ed.* **50**, 1000–1045 (2011).
- E. Havinga, J. L. M. A. Schlatmann, *Tetrahedron* **16**, 146–152 (1961).
- J. E. Baldwin, S. M. Krueger, *J. Am. Chem. Soc.* **91**, 6444–6447 (1969).
- M. M. de Christo Scherer *et al.*, *J. Tissue Viability* **28**, 94–99 (2019).
- W. G. Dauben, J. Rabinowitz, N. D. Vietmeyer, P. H. Wendschuh, *J. Am. Chem. Soc.* **94**, 4285–4292 (1972).
- C. W. Spangler, R. P. Hennis, *Chem. Commun.* **1972**, 24–25 (1972).
- M. K. Lawless, S. D. Wickham, R. A. Mathies, *Acc. Chem. Res.* **28**, 493–502 (1995).
- P. J. Reid, S. J. Doig, R. A. Mathies, *J. Phys. Chem.* **94**, 8396–8399 (1990).
- M. Garavelli *et al.*, *J. Phys. Chem. A* **105**, 4458–4469 (2001).
- B. C. Arruda, B. Smith, K. G. Spears, R. J. Senson, *Faraday Discuss.* **163**, 159–171 (2013).
- O. Njoya, S. Matsika, T. Weinacht, *ChemPhysChem* **14**, 1451–1455 (2013).
- B. C. Arruda, R. J. Senson, *Phys. Chem. Chem. Phys.* **16**, 4439–4455 (2014).

- M. Ben-Nun, T. J. Martínez, *Adv. Chem. Phys.* **121**, 439–512 (2002).
- M. Ben-Nun, T. J. Martínez, *J. Chem. Phys.* **108**, 7244–7257 (1998).
- M. Ben-Nun, J. Quenneville, T. J. Martínez, *J. Phys. Chem. A* **104**, 5161–5175 (2000).
- S. Matsika, P. Krause, *Annu. Rev. Phys. Chem.* **62**, 621–643 (2011).
- A. Hofmann, R. de Vivie-Riedle, *Chem. Phys. Lett.* **346**, 299–304 (2001).
- K. M. Marzec, I. Reva, R. Fausto, L. M. Proniewicz, *J. Phys. Chem. A* **115**, 4342–4353 (2011).
- J. W. Snyder Jr., R. M. Parrish, T. J. Martínez, *J. Phys. Chem. Lett.* **8**, 2432–2437 (2017).
- T. J. A. Wolf *et al.*, *Nat. Chem.* **11**, 504–509 (2019).
- M. H. Kim, L. Shen, H. Tao, T. J. Martínez, A. G. Suits, *Science* **315**, 1561–1565 (2007).
- S. T. Park, S. K. Kim, M. S. Kim, *Nature* **415**, 306–308 (2002).
- K.-W. Choi, D.-S. Ahn, J.-H. Lee, S. K. Kim, *Chem. Commun.* **2007**, 1041–1043 (2007).
- F. Filsinger, G. Meijer, H. Stapelfeldt, H. N. Chapman, J. Küpper, *Phys. Chem. Chem. Phys.* **13**, 2076–2087 (2011).
- Y.-P. Chang, D. A. Horke, S. Trippel, J. Küpper, *Int. Rev. Phys. Chem.* **34**, 557–590 (2015).
- T. Endo *et al.*, *Science* **370**, 1072–1077 (2020).
- T. J. A. Wolf, Figures for “Conformer-specific photochemistry imaged in real space and time”. DOI:10.5281/zenodo.5214798.

ACKNOWLEDGMENTS

We thank J. P. Cryan, M. C. Hoffmann, R. K. Li, M. Niebuhr, S. Weathersby, and T. Weinacht for their help and fruitful discussions. Lawrence Livermore National Laboratory is operated by Lawrence Livermore National Security, LLC, for the US Department of Energy (DOE), National Nuclear Security Administration, under contract DE-AC52-07NA27344. **Funding:** This work was supported by the AMOS program within the DOE Office of Science, Basic Energy Sciences, Chemical Sciences, Geosciences, and Biosciences Division. The experimental part of this research was performed at the SLAC MeV UED facility, which is supported in part by the DOE BES SUF Division Accelerator & Detector

R&D program, the Linac Coherent Light Source (LCLS) Facility, and SLAC under contracts DE-AC02-05-CH11231 and DE-AC02-76SF00515. Also supported by a Volkswagen Foundation Lichtenberg Professorship (M.G.); a NSF graduate fellowship (D.M.S.); and DOE Office of Science, Basic Energy Sciences awards DE-SC0014170 (J.P.F.N. and M.C.) and DE-FG02-08ER15984 (Y.L.). **Author contributions:** Conceptualization: D.M.S., T.J.M., and T.J.A.W. Methodology: J.Y., J.P.F.N., M.C., M.G., B.M., X.S., X.J.W., and T.J.A.W. Investigation: E.G.C., D.M.S., J.Y., J.P.F.N., A.A., M.C., R.F., M.G., K.H., F.J., S.K.S., Y.L., M.-F.L., D.L., B.M., X.S., M.R.W., X.J.W., T.J.M., and T.J.A.W. Visualization: E.G.C., D.M.S., and T.J.A.W. Funding acquisition: M.C., M.G., X.J.W.,

T.J.M., and T.J.A.W. Project administration: T.J.A.W. Supervision: T.J.M. and T.J.A.W. Writing—original draft: E.G.C., D.M.S., T.J.M., and T.J.A.W. Writing—review and editing: E.G.C., D.M.S., J.Y., J.P.F.N., A.A., M.C., R.F., M.G., K.H., F.J., S.K.S., Y.L., M.-F.L., D.L., B.M., X.S., M.R.W., X.J.W., T.J.M., and T.J.A.W. **Competing interests:** None declared. **Data and materials availability:** All data underlying the figures are deposited in the Zenodo repository (30). The raw experimental data are archived at the SLAC MeV-UED facility, and the raw simulated data are stored at the Martinez laboratory at Stanford University and SLAC. All data needed to evaluate the conclusions in the paper are present in the paper or the supplementary materials.

SUPPLEMENTARY MATERIALS

science.org/doi/10.1126/science.abk3132
Materials and Methods
Supplementary Text
Figs. S1 to S15
Tables S1 to S3
References (31–41)
Movies S1 to S26

6 July 2021; accepted 24 August 2021
[10.1126/science.abk3132](https://doi.org/10.1126/science.abk3132)

Conformer-specific photochemistry imaged in real space and time

E. G. Champenois D. M. Sanchez J. Yang J. P. Figueira Nunes A. Attar M. Centurion R. Forbes M. Gühr K. Hegazy F. Ji S. K. Saha Y. Liu M.-F. Lin D. Luo B. Moore X. Shen M. R. Ware X. J. Wang T. J. Martínez T. J. A. Wolf

Science, 374 (6564), • DOI: 10.1126/science.abk3132

Conformer-specific dynamics

Conformation-dependent dynamics play an important role in organic chemistry syntheses such as electrocyclic reactions, as well as in biological processes such as protein folding. However, current time-resolved experimental methods struggle to distinguish conformers from each other, and conformational isomerism is usually analyzed through reactant and product distributions. Using a combination of mega-electron volt ultrafast electron diffraction and quantum wave packet simulations, Champenois *et al.* directly followed the photochemical electrocyclic ring opening of the molecule β -phellandrene with femtosecond time resolution and confirmed that the transformation of a specific molecular conformer follows the famous Woodward-Hoffmann rules. The proposed method is potentially a powerful tool to follow conformer specificity in various organic and biological systems in real time. —YS

View the article online

<https://www.science.org/doi/10.1126/science.abk3132>

Permissions

<https://www.science.org/help/reprints-and-permissions>

Use of this article is subject to the [Terms of service](#)

Science (ISSN) is published by the American Association for the Advancement of Science, 1200 New York Avenue NW, Washington, DC 20005. The title *Science* is a registered trademark of AAAS.

Copyright © 2021 The Authors, some rights reserved; exclusive licensee American Association for the Advancement of Science. No claim to original U.S. Government Works